HHS Public Access

Author manuscript

Nat Med. Author manuscript; available in PMC 2015 July 01.

Published in final edited form as:

Nat Med. 2015 January ; 21(1): 76–80. doi:10.1038/nm.3710.

Inducible depletion of satellite cells in adult, sedentary mice impairs muscle regenerative capacity but does not contribute to sarcopenia

Christopher S. Fry[1,2], **Jonah D. Lee**[1,2], **Jyothi Mula**[1,2], **Tyler J. Kirby**[2,3], **Janna R. Jackson**[1,2], **Fujun Liu**[2,4], **Lin Yang**[2,4], **Christopher L. Mendias**[5], **Esther E. Dupont-Versteegden**[1,2], **John J. McCarthy**[2,3,†], and **Charlotte A. Peterson**[1,2,3,*,†]

[1]Department of Rehabilitation Sciences, College of Health Sciences University of Kentucky, Lexington, Kentucky 40536, USA.

[2]Center for Muscle Biology University of Kentucky, Lexington, Kentucky 40536, USA.

[3]Department of Physiology, College of Medicine University of Kentucky, Lexington, Kentucky 40536, USA.

[4]Department of Biostatistics, College of Public Health University of Kentucky, Lexington, Kentucky 40536, USA.

[5]Department of Orthopaedic Surgery University of Michigan, Ann Arbor, MI 48109, USA

A key determinant of geriatric frailty is sarcopenia, the age-associated loss of skeletal muscle mass and strength[1,2]. Although the etiology of sarcopenia is unknown, the correlation between the loss of satellite cell activity and impaired regenerative capacity in aged muscle has led to the hypothesis that diminished activity of satellite cells, or skeletal muscle stem cells, with age is a cause of sarcopenia[3,4]. We tested this hypothesis using a mouse model to deplete young adult muscle of satellite cells to a level sufficient to impair regeneration throughout the life of the animal. A detailed analysis of multiple muscles in sedentary male mice revealed that, despite reduced regenerative capacity, the life-long reduction of satellite cells did not accelerate nor exacerbate sarcopenia. These data argue against satellite cell contribution to the maintenance of muscle size or fiber type composition during aging; however, an increase in extracellular matrix suggests that loss of satellite cells may contribute to fibrosis with age.

Recent estimates indicate that up to one-third of the elderly suffer from frailty, characterized by a common set of symptoms including loss of muscle strength, increased fatigability, modest levels of physical activity and decreased body weight[1]. The close relationship

*Correspondence to: 900 S. Limestone, CTW 105 University of Kentucky Lexington, KY 40536 Tel: 859-218-0476 Fax: 859-257-2375 cpete4@uky.edu.

†Co-senior authors

Author Contributions C.S.F, J.D.L., J.J.M and C.A.P. designed the study. C.S.F, J.D.L., J.M., T.J.K., J.R.J., and C.L.M. performed experiments and collected the data. C.S.F, J.D.L., J.M., F.L., L.Y., C.L.M. and E.E.D. analyzed the data. C.S.F, J.J.M and C.A.P. wrote the manuscript. All authors approved the final version of the manuscript.

between frailty and the musculoskeletal system suggests sarcopenia is a critical factor contributing to the emergence of geriatric frailty, thus limiting the ability to perform activities of daily living and significantly increasing the risk of falling [5,6]. Numerous studies in humans and rodents report a strong correlation between the loss and dysfunction of satellite cells and sarcopenia [3,4]. Motivated by the idea that the restoration of satellite cell activity will provide a therapeutic basis for treating sarcopenia, a great deal of effort has gone into defining the environmental and cellular changes underlying the loss in satellite cell activity with age[7-18]. Despite the correlation between declining satellite cell-dependent regenerative capacity and age, no studies to date have tested this relationship to determine if the loss of satellite cell activity causes sarcopenia. We recently developed a genetic mouse model that allows for the specific, inducible depletion of satellite cells in adult skeletal muscle[19-21]. The $Pax7^{CreER/+}$; $Rosa26^{DTA/+}$ strain, designated $Pax7^{CreER}$-DTA, was generated by crossing $Pax7^{CreER/CreER}$ and $Rosa26^{DTA/DTA}$ strains. Treatment of the $Pax7^{CreER}$-DTA mouse with tamoxifen activates *Cre* recombinase only in satellite cells driven by the *Pax7* promoter, which activates the diphtheria toxin A gene, killing satellite cells[21]. We took advantage of this mouse model to directly test the hypothesis that loss of satellite cells, which underlies the well-documented impairment in muscle regenerative capacity[21-24], results in muscle wasting with advancing age. If there is a causal relationship between the loss of satellite cell activity and sarcopenia, then we would predict accelerated and exacerbated sarcopenia in muscle with a significantly reduced complement of satellite cells.

We administered vehicle or tamoxifen by IP injection to adult (4 months of age) male $Pax7^{CreER}$ -DTA mice for five consecutive days to effectively deplete satellite cells and then allowed the mice to age. We analyzed a subset of mice after approximately one year, at 16–18 months of age (middle age, MA), and showed that satellite cell numbers did not recover over time. Consistent with previous studies[21,23], in muscles which remained significantly satellite cell-depleted (>85%), muscle regeneration following $BaCl_2$ injection was severely impaired (Fig. 1a). No loss of muscle mass was apparent in any hind limb muscle of vehicle- or tamoxifen-treated middle aged mice except in the soleus muscle (MA, Fig.1b); however, significant atrophy was apparent by 24 months in both vehicle- and tamoxifen-treated mice (Aged, Fig. 1b). Decrements in hind limb muscle mass in the aged mice met criteria for sarcopenia in humans[25]; that is, appendicular muscle mass was two standard deviations below the young group. Thus, loss of satellite cell-dependent regenerative capacity throughout adulthood does not accelerate sarcopenia in aging mice.

We next determined if in aged mice, features of sarcopenia were exacerbated due to a lifetime reduction of satellite cells. Analysis of satellite cell abundance in vehicle-treated 5 month old (1 month following injection, young, Fig. 2a) and 24 month old (20 months following injection, aged, Fig. 2a) mice showed a substantial age-associated reduction in satellite cells (Fig. 2b). Tamoxifen administration resulted in >94% reduction in satellite cells in multiple hind limb muscles 1 month following injection, with little recovery in satellite cells per myofiber occurring even after 20 months (Fig. 2b); on average, satellite cells remained 83% depleted in aged mice (range: 64-87%), well below the loss normally associated with aging. Despite the reduction in satellite cell abundance to levels associated

with severely impaired muscle regeneration, age-associated atrophy, as indicated both by muscle wet weight (Fig. 1b) and by mean myofiber cross-sectional area (CSA, Fig. 2c), occurred to the same extent in all hind limb muscles from both vehicle-treated and satellite cell-depleted mice. Myofiber CSA analyzed by fiber type (Figs. 3a and b) showed age-related atrophy in all muscles except the soleus, which has a higher proportion of slow-twitch fibers (Fig. 3c). In agreement with the well-characterized atrophy of the largest, fast-twitch glycolytic fibers with age[26], type 2b fibers showed the greatest degree of atrophy that was unaffected by satellite cell abundance (Fig. 3c). Moreover, fiber size distribution across hind limb muscles showed the characteristic leftward shift due to overall higher abundance of smaller fibers with age in both treatment groups (Supplemental Fig. 1). Satellite cell depletion also had no significant effect on fiber type distribution (Supplemental Fig. 2); at 24 months, only the plantaris and soleus muscles showed an age-dependent shift in the relative frequency of different fast-twitch (type 2) fibers that was independent of satellite cell abundance.

In addition to atrophy of individual myofibers, sarcopenia is associated with a decline in the number of myofibers and a reduction in single fiber specific force generation (force per unit area)[2]. We measured these characteristics in the plantaris muscle, as it showed little recovery of satellite cells with age and was therefore most severely depleted (see Fig. 2b). We did not observe a loss of myofibers at 24 months in either vehicle- or tamoxifen-treated mice (Fig. 4a). Analyses of isolated myofibers (Fig. 4b) showed that the number of myonuclei per 100 μm of myofiber length was not changed with age (Fig. 4c). We performed myonuclear counts primarily on intermediate-sized myofibers (1000–2500 μm^2), that make up greater than 80% of all myofibers, and our results are consistent with a recent study reporting no myonuclear loss with age in fibers in this size range[27]. Moreover, myonuclear number was unaffected by satellite cell depletion (Fig. 4c), suggesting that the maintenance of myonuclei is not linked to satellite cell abundance. This conclusion was further supported by analysis of BrdU-labeled myonuclei (Fig. 4d). We provided mice with BrdU via drinking water for two weeks prior to sacrifice, and quantified fusion of labeled nuclei into myofibers. Although myonuclear addition was very infrequent during the two week labeling (approximately 0.1% of myofibers from vehicle-treated young and aged mice contained a labeled myonucleus), no labeled myonuclei were detected in plantaris muscle following tamoxifen treatment (Fig. 4d). Finally, as shown in Fig. 4e, myofiber specific force was reduced 31% with age, comparable to the force decrement reported in isolated myofibers in adult humans aged 65–85 years, using a similar permeabilized fiber preparation[28]; however, the decrease in specific force was unaffected by satellite cell abundance. We also functionally tested single fibers from the EDL muscle from 24 month old tamoxifen- and vehicle-treated mice (Supplemental Fig. 3a–c). As with the plantaris muscle, neither specific or absolute force, nor single fiber CSA, were affected by satellite cell depletion in the EDL. Further, overall loss of function with age, as measured by grip strength, was not altered by satellite cell depletion (Supplemental Fig. 3d). The loss of 45–59% raw grip strength in the aged mice did not differ with treatment, and is consistent with loss reported in humans with age [29,30].

Although age-related myofiber atrophy and weakness were not altered by lifelong satellite cell reduction, we did observe a change in the muscle fiber environment. Extracellular matrix (ECM) surrounding myofibers, quantified by Sirius Red staining of collagens, was

higher with age and reduced satellite cell content in the plantaris muscle (representative images, Fig. 4f and g, quantified in Fig. 4h). We also assessed ECM accumulation via alpha-wheat germ agglutinin (WGA) staining of glycosaminoglycans, which showed that this component of the ECM was also more abundant with age and satellite cell depletion (representative images Supplemental Fig. 4a and b, quantified in Supplemental Fig. 4c). WGA staining of other hind limb muscles showed excess accumulation of ECM with age that was further exacerbated by a reduction in satellite cell content specifically in the plantaris and TA/EDL muscles (Supplemental Fig. 4c). These observations support our recent findings that satellite cells regulate the myofiber environment by signaling to fibroblasts[19]. While our previous work illustrated an additive effect of satellite cell-depletion and functional overload on ECM deposition in young adult mice[19], novel findings in the current study show that long term depletion of satellite cells in sedentary mice contributes to dysregulation of the ECM in old age. Moreover, the present work extends previous findings to suggest that satellite cells may limit fibrosis preferentially in fast muscles[31].

In summary, although our understanding of satellite cell function in muscle regeneration continues to be refined, the present study provides convincing evidence that the loss of satellite cell-dependent regenerative capacity neither accelerates nor exacerbates sarcopenia. Moreover, our findings have broader implications for the study of tissue homeostasis by showing that skeletal muscle, much like the pancreas, kidney and liver, apparently employs cellular mechanisms that do not necessarily require stem cell participation for tissue maintenance[32-35]. However, the loss of satellite cells may adversely affect overall muscle quality, potentially contributing to the increase in fibrosis observed in aged skeletal muscle[12]. One limitation of the current findings stems from the sedentary nature of the mice. The satellite cell requirement for muscle maintenance in more physically active mice remains to be determined; however, the sedentary nature of the mice in the current study is reflective of low physical activity levels of older adults in the United States[36]. The findings of the current study have clinical importance as they draw a clear distinction between therapeutic strategies that may effectively treat degenerative myopathies, such as dystrophies[37] and cachexia[38], versus sarcopenia. While degenerative conditions are expected to benefit from a satellite cell-based therapy, our results support the conclusion of a recent study[39], that treatment for sarcopenia should more appropriately focus on the myofiber and motor neuron.

Online Methods

Mouse Model

The Pax7^{CreER}-DTA genetic mouse model allows for the specific and inducible depletion of satellite cells upon tamoxifen treatment, through activation of the diphtheria toxin A gene only in Pax7-expressing cells [21]. The Pax7^{CreER} strain was generated by placing an *ires-CreERTM-FRT-Neo-FRT* cassette into the *Cla*I site of the Pax7 gene 3′-UTR following the stop codon in exon 9 [40]. Mice are on a mixed C57BL/6 – 129 background strain. All animal procedures were conducted in accordance with institutional guidelines approved by the Institutional Animal Care and Use Committee of the University of Kentucky. Mice were housed in a temperature- and humidity-controlled room and maintained on a 14:10 h light:

dark cycle with food and water *ad libitum*. Mice were not housed in a barrier/pathogen-free facility, and were not screened for tumors. Sample size was determined by a power analysis with an expected standard deviation of 0.001, power of 0.8 and alpha of 0.05. Adult (4 months of age), male $Pax7^{CreER}$-DTA mice were randomized and administered by intraperitoneal (IP) injection either vehicle (15% ethanol in sunflower seed oil) or tamoxifen ($2.0\ mg \cdot d^{-1}$) for five consecutive days, two hours prior to lights out. Following one month (5 month old, young), 12 months (16–18 month old, middle aged (MA)) or 20 months (24 month old, aged), vehicle and tamoxifen-treated mice were sacrificed (n=4–8 mice/group). Aged vehicle mice had a median lifespan of 23.9 months, and a maximum lifespan of 24.6 months; aged tamoxifen mice had a median lifespan of 22.6 months and a maximum lifespan of 24.4 months. A subset of mice was provided with 5-bromo-2′-deoxyuridine (BrdU) at a concentration of $0.8\ mg \cdot ml^{-1}$ in their drinking water for two weeks prior to sacrifice.

$BaCl_2$-induced muscle injury

MA mice were anesthetized with isoflurane and the tibialis anterior (TA) injected with either 50 μl of 1.2% $BaCl_2$ solution or sterile PBS. After seven days, TA muscles were collected and processed for histochemistry.

Histochemistry/Immunohistochemistry

Muscles were mounted at resting length, covered in OCT compound and frozen in liquid nitrogen-cooled isopentane and stored at −80 °C until cryosectioning (7μm). For Pax7 (satellite cells) immunohistochemistry, muscle sections were fixed in 4% paraformaldehyde (PFA) followed by epitope retrieval using sodium citrate (10 mM, pH 6.5) at 92 °C for 20 min. Endogenous peroxidase activity was blocked with 3% hydrogen peroxide in phosphate-buffered saline followed by an additional blocking step with Mouse-on-Mouse Blocking Reagent (Vector Laboratories, Burlingame, CA). Incubation with Pax7 antibody (1:100, Developmental Studies Hybridoma Bank, Iowa City, IA) was followed by incubation with the biotin-conjugated secondary antibody and streptavidin-HRP included within the Tyramide Signal Amplification kit (Cat#T20935, Invitrogen, Carlsbad, CA). Sections were co-stained with DAPI (4′, 6′-diamidino-2-henylindole, 10 nM, Invitrogen), and mounted with Vectashield fluorescent mounting media. For fiber typing, unfixed sections were incubated in antibodies against myosin heavy chain (MyHC) types 1, 2a and 2b (1:100, Cat#BA.D5, SC.71 and BF.F3, Developmental Studies Hybridoma Bank) in addition to dystrophin (1:50, Cat#VPD505, Vector). MyHC type 2x expression was assumed from unstained fibers. Fluorescent-conjugated secondary antibodies against various mouse immunoglobulin subtypes were applied to visualize MyHC expression and dystrophin. Sections were post-fixed in 4% PFA prior to mounting. For extracellular matrix accumulation, muscle sections were fixed in 4% PFA, and then incubated with Texas-red conjugated WGA (wheat germ agglutinin, Cat#W21405, Invitrogen). Basic muscle morphology and regeneration were assessed with hematoxylin and eosin staining, and collagen content was assessed with Sirius Red staining following standard protocols. For BrdU detection, unfixed slides were incubated in an antibody against dystrophin followed by secondary antibody conjugated to Texas-Red (Cat#610-109-121, Rockland Immunochemicals Inc., Gilbertsville, PA). Sections were then fixed in absolute methanol,

treated with 2 N HCl to denature DNA and neutralized with 0.1 M borate buffer (BORAX, pH 8.5). BrdU antibody incubation was followed by biotin-conjugated goat anti-mouse secondary antibody and streptavidin-FITC (Cat#SA-5001, Vector). Sections were postfixed in PFA and co-stained with DAPI.

Image Quantification

Images were captured at 10 and 20x with an upright microscope (AxioImager M1; Zeiss, Göttingen, Germany). Fiber type-specific cross-sectional area was quantified using a newly developed, automated image segmentation algorithm [41,42], that identifies fiber types by MyHC isoform expression combined with fiber boundary detection using dystrophin immunohistochemistry. All other images were quantified with Zeiss Axiovision rel. software (v4.8). Satellite cell abundance was assessed using Pax7 staining and only those cells that were Pax7+ and DAPI+ were counted. Fibers were classified as BrdU+ with a BrdU+/DAPI+ nucleus within the dystrophin border. WGA and Sirius Red staining were quantified using threshold intensity programs within the imaging software. Investigators were blinded to treatment (vehicle/tamoxifen) but not age during image quantification and analysis.

Single Myofiber Contractility

Measurement of permeabilized muscle fiber contractility was performed as previously described [43]. Muscles were removed from the animal and immediately placed in ice cold relaxing solution. Bundles of fibers were dissected from whole muscles, placed in skinning solution for 30 min and then in storage solution for 16 h at 4 °C and assayed immediately or stored at −80 °C until use. Individual myofibers (n=8 myofibers/mouse; 3-8 mice/group; see figure legends for specific numbers) were pulled from bundles in relaxing solution and secured at one end to a force transducer (Aurora Scientific, Model 403, Ontario, Canada) and at the other end to a servomotor (Aurora Scientific). The length of the whole fiber was adjusted to obtain a sarcomere length of 2.5μm using laser diffraction techniques. The average fiber cross-sectional area (CSA) was calculated assuming an elliptical cross-section, with diameters obtained at five different positions along the fiber from high-magnification images of the top and the side views. Maximum isometric force (F_o) of the fiber was elicited by immersing the fiber in a high-Ca^{2+} concentration solution. Specific force (sF_o) was calculated by dividing F_o by CSA.

Myonuclear Number

Plantaris muscles were fixed *in situ* at resting length in 4% PFA for 48 h. Single myofibers were isolated by 40% NaOH digestion, as previously described [21]. Single myofibers were stained with DAPI and nuclei from 15–25 myofibers per animal (n = 4–8 mice/group) within a given segment were counted by *z*-stack analysis using the AxioImager M1 microscope. AxioVision software was used to measure myonuclear number per myofiber segment.

Grip Strength

Mice were held at the base of the tail and were allowed to grab with fore limb paws the horizontal bar of the grip strength apparatus in a pronated manner (Columbus Instruments,

Columbus, OH) while being held horizontally. The mice were then pulled back gently until the grip was released and the maximal force achieved by the animal was recorded (in N); hind limbs were kept free from the apparatus and the average of 3 trials was reported. Data are presented as mean grip strength per body weight. All mice were tested by the same person.

Statistics

All data were analyzed with SigmaPlot v12.0 software (Systat Software, San Jose, CA) via a two-factor ANOVA (vehicle/tamoxifen x young/MA/aged) or (vehicle/tamoxifen x young/aged) or simple two-tailed t-tests for each dependent variable under consideration. Assumptions for statistical analyses were met (i.e. normal distribution, equal variance). If a significant interaction was detected, an appropriate *post-hoc* analysis was employed to determine the source of the significance. Statistical significance was accepted at $P < 0.05$. Data are reported as mean ± standard error.

Supplementary Material

Refer to Web version on PubMed Central for supplementary material.

Acknowledgments

The authors thank Ben Lawson and Ken Campbell from the University of Kentucky Center for Muscle Biology, and Stuart Roche from University of Michigan for technical assistance on single fiber functional analyses; Catherine Starnes for her biostatistics expertise; Thomas Chaillou for assistance with muscle regeneration experiments; Amy Confides for assistance with grip strength testing; and Margo Ubele, Rod Erfani, Jake Beggs, Marilyn Campbell, Tyler Kmiec, Justin Werker, Robin Anglin and Zakkary Hardyniec for image acquisition and quantification. Research was supported by the Jeane B. Kempner Postdoctoral Scholar Award and NIH grant AR065337 to C.S.F.; Ellison Medical Foundation/American Federation of Aging Research Fellow EPD 12102 to J.D.L.; NIH grants AG34453 to C.A.P., AG043721 to E.E.D., and AR60701 to C.A.P. and J.J.M.; and the NIH National Center for Advancing Translational Sciences, through Grant UL1TR000117. The content is solely the responsibility of the authors and does not necessarily represent the official views of the NIH or AFAR.

References

1. Bortz WM 2nd. A conceptual framework of frailty: a review. J Gerontol A Biol Sci Med Sci. 2002; 57:M283–288. [PubMed: 11983721]
2. Mitchell WK, et al. Sarcopenia, dynapenia, and the impact of advancing age on human skeletal muscle size and strength; a quantitative review. Front Physiol. 2012; 3:260. [PubMed: 22934016]
3. Garcia-Prat L, Sousa-Victor P, Munoz-Canoves P. Functional dysregulation of stem cells during aging: a focus on skeletal muscle stem cells. FEBS J. 2013; 280:4051–4062. [PubMed: 23452120]
4. Gopinath SD, Rando TA. Stem cell review series: aging of the skeletal muscle stem cell niche. Aging Cell. 2008; 7:590–598. [PubMed: 18462272]
5. Topinkova E. Aging, disability and frailty. Ann Nutr Metab. 2008; 52(Suppl 1):6–11. [PubMed: 18382070]
6. Walston J, et al. Research agenda for frailty in older adults: toward a better understanding of physiology and etiology: summary from the American Geriatrics Society/National Institute on Aging Research Conference on Frailty in Older Adults. J Am Geriat Soc. 2006; 54:991–1001. [PubMed: 16776798]
7. Sinha M, et al. Restoring systemic GDF11 levels reverses age-related dysfunction in mouse skeletal muscle. Science. 2014; 344:649–652. [PubMed: 24797481]
8. Collins CA, Zammit PS, Ruiz AP, Morgan JE, Partridge TA. A population of myogenic stem cells that survives skeletal muscle aging. Stem Cell. 2007; 25:885–894.

9. Shefer G, Van de Mark DP, Richardson JB, Yablonka-Reuveni Z. Satellite-cell pool size does matter: defining the myogenic potency of aging skeletal muscle. Dev Biol. 2006; 294:50–66. [PubMed: 16554047]
10. Chakkalakal JV, Jones KM, Basson MA, Brack AS. The aged niche disrupts muscle stem cell quiescence. Nature. 2012; 490:355–360. [PubMed: 23023126]
11. Bernet JD, et al. p38 MAPK signaling underlies a cell-autonomous loss of stem cell self-renewal in skeletal muscle of aged mice. Nat Med. 2014
12. Brack AS, et al. Increased Wnt signaling during aging alters muscle stem cell fate and increases fibrosis. Science. 2007; 317:807–810. [PubMed: 17690295]
13. Carlson ME, Conboy IM. Loss of stem cell regenerative capacity within aged niches. Aging Cell. 2007; 6:371–382. [PubMed: 17381551]
14. Conboy IM, et al. Rejuvenation of aged progenitor cells by exposure to a young systemic environment. Nature. 2005; 433:760–764. [PubMed: 15716955]
15. Cosgrove BD, et al. Rejuvenation of the muscle stem cell population restores strength to injured aged muscles. Nat Med. 2014
16. McKay BR, et al. Elevated SOCS3 and altered IL-6 signaling is associated with age-related human muscle stem cell dysfunction. Am J Physiol Cell Physiol. 2013; 304:C717–728. [PubMed: 23392112]
17. Shefer G, Rauner G, Yablonka-Reuveni Z, Benayahu D. Reduced satellite cell numbers and myogenic capacity in aging can be alleviated by endurance exercise. PLoS One. 2010; 5:e13307. [PubMed: 20967266]
18. Sousa-Victor P, et al. Geriatric muscle stem cells switch reversible quiescence into senescence. Nature. 2014; 506:316–321. [PubMed: 24522534]
19. Fry CS, et al. Regulation of the muscle fiber microenvironment by activated satellite cells during hypertrophy. FASEB J. 2014; 28:1654–65. [PubMed: 24376025]
20. Jackson JR, et al. Satellite cell depletion does not inhibit adult skeletal muscle regrowth following unloading-induced atrophy. Am J Physiol Cell Physiol. 2012; 303:C854–861. [PubMed: 22895262]
21. McCarthy JJ, et al. Effective fiber hypertrophy in satellite cell-depleted skeletal muscle. Development. 2011; 138:3657–3666. [PubMed: 21828094]
22. Lepper C, Partridge TA, Fan CM. An absolute requirement for Pax7-positive satellite cells in acute injury-induced skeletal muscle regeneration. Development. 2011; 138:3639–3646. [PubMed: 21828092]
23. Murphy MM, Lawson JA, Mathew SJ, Hutcheson DA, Kardon G. Satellite cells, connective tissue fibroblasts and their interactions are crucial for muscle regeneration. Development. 2011; 138:3625–3637. [PubMed: 21828091]
24. Sambasivan R, et al. Pax7-expressing satellite cells are indispensable for adult skeletal muscle regeneration. Development. 2011; 138:3647–3656. [PubMed: 21828093]
25. Baumgartner RN, et al. Epidemiology of sarcopenia among the elderly in New Mexico. Am J Epidemiol. 1998; 147:755–763. [PubMed: 9554417]
26. Larsson L. Motor units - remodeling in aged animals. J Gerontol A Biol Sci Med Sci. 1995; 50:91–95. [PubMed: 7493226]
27. Brack AS, Bildsoe H, Hughes SM. Evidence that satellite cell decrement contributes to preferential decline in nuclear number from large fibres during murine age-related muscle atrophy. J Cell Sci. 2005; 118:4813–4821. [PubMed: 16219688]
28. Yu F, Hedstrom M, Cristea A, Dalen N, Larsson L. Effects of ageing and gender on contractile properties in human skeletal muscle and single fibres. Acta Physiol. 2007; 190:229–241.
29. Sinaki M, Nwaogwugwu NC, Phillips BE, Mokri M. Effect of gender, age, and anthropometry on axial and appendicular muscle strength. Am J Phys Med Rehab. 2001; 80:330–338.
30. Shephard RJ, Montelpare W, Plyley M, McCracken D, Goode RC. Handgrip dynamometry, Cybex measurements and lean mass as markers of the ageing of muscle function. Br J Sports Med. 1991; 25:204–208. [PubMed: 1810614]

31. Morrison J, Lu QL, Pastoret C, Partridge T, Bou-Gharios G. T-cell-dependent fibrosis in the mdx dystrophic mouse. Lab Investig. 2000; 80:881–891. [PubMed: 10879739]
32. Dor Y, Brown J, Martinez OI, Melton DA. Adult pancreatic beta-cells are formed by self-duplication rather than stem-cell differentiation. Nature. 2004; 429:41–46. [PubMed: 15129273]
33. Humphreys BD, et al. Intrinsic epithelial cells repair the kidney after injury. Cell Stem Cell. 2008; 2:284–291. [PubMed: 18371453]
34. Miyaoka Y, et al. Hypertrophy and Unconventional Cell Division of Hepatocytes Underlie Liver Regeneration. Curr Biol. 2012; 22:1166–1175. [PubMed: 22658593]
35. Teta M, Rankin MM, Long SY, Stein GM, Kushner JA. Growth and regeneration of adult beta cells does not involve specialized progenitors. Dev Cell. 2007; 12:817–826. [PubMed: 17488631]
36. Jones DA, et al. Moderate leisure-time physical activity: who is meeting the public health recommendations? A national cross-sectional study. Arch Fam Med. 1998; 7:285–289. [PubMed: 9596466]
37. Law PK, et al. Feasibility, safety, and efficacy of myoblast transfer therapy on Duchenne muscular dystrophy boys. Cell Transplant. 1992; 1:235–244. [PubMed: 1344295]
38. He WA, et al. NF-kappaB-mediated Pax7 dysregulation in the muscle microenvironment promotes cancer cachexia. J Clin Investig. 2013; 123:4821–4835. [PubMed: 24084740]
39. Bareja A, Billin AN. Satellite cell therapy - from mice to men. Skelet Muscle. 2013; 3:2. [PubMed: 23369649]

Online Methods References

40. Nishijo K, et al. Biomarker system for studying muscle, stem cells, and cancer in vivo. FASEB J. 2009; 23:2681–2690. [PubMed: 19332644]
41. Mula J, Lee JD, Liu F, Yang L, Peterson CA. Automated image analysis of skeletal muscle fiber cross-sectional area. J Appl Physiol. 2013; 114:148–155. [PubMed: 23139362]
42. Liu F, et al. Automated fiber-type-specific cross-sectional area assessment and myonuclei counting in skeletal muscle. J Appl Physiol. 2013; 115:1714–1724. [PubMed: 24092696]
43. Mendias CL, Kayupov E, Bradley JR, Brooks SV, Claflin DR. Decreased specific force and power production of muscle fibers from myostatin-deficient mice are associated with a suppression of protein degradation. J Appl Physiol. 2011; 111:185–191. [PubMed: 21565991]

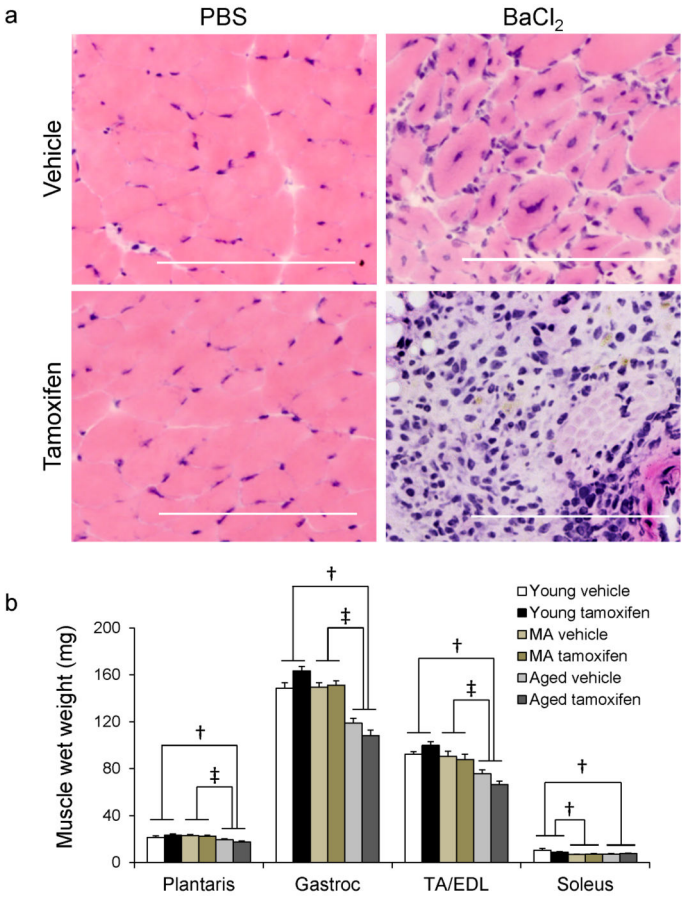

Figure 1. Reduction in satellite cell content leads to impaired regenerative capacity but not accelerated or exacerbated sarcopenia

(**a**) Tibialis anterior muscles of vehicle- and tamoxifen-treated Pax7^{CreER}-DTA middle aged (MA, 16-18 month) mice following barium chloride ($BaCl_2$) or PBS injection. Hematoxylin and eosin stained cross-sections 7 days after injection. Scale bar = 100 μm. (**b**) Hind limb muscle (plantaris, gastrocnemius (gastroc), tibialis anterior/extensor digitorum longus (TA/EDL), soleus) wet weights. Data are presented as mean weight (mg) ± SEM. n = 4–8 mice/group. † Significantly different than young mice ($P < 0.05$), ‡ Significantly different than MA mice ($P < 0.05$) as measured by a two-way ANOVA (factors: young/aged and vehicle/tamoxifen).

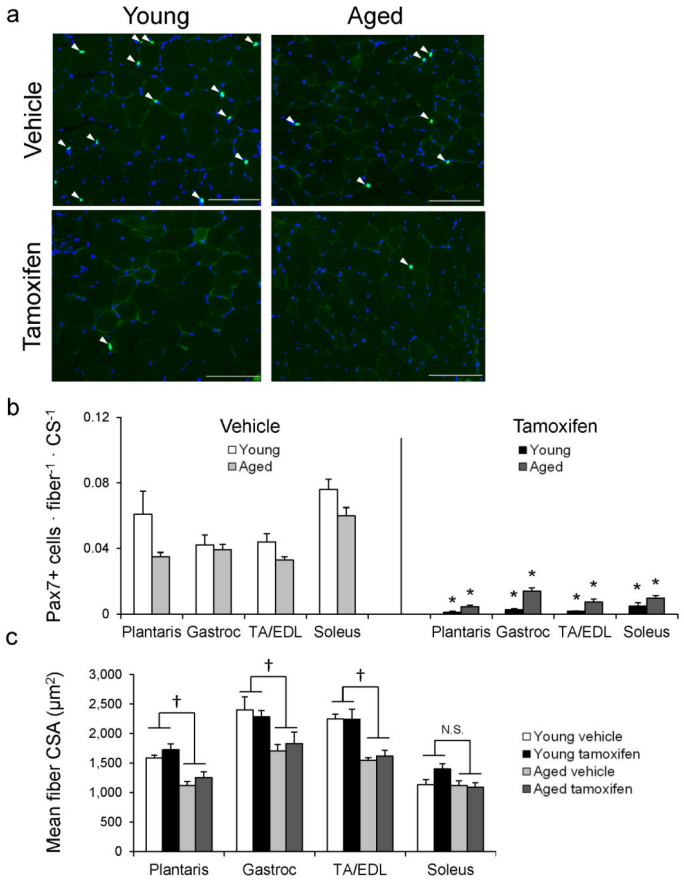

Figure 2. Reduction in satellite cell content throughout the lifespan does not affect mean myofiber cross-sectional area (CSA)

(**a**) Satellite cell quantification of plantaris, gastrocnemius, TA/EDL and soleus muscles of vehicle- and tamoxifen-treated Pax7^{CreER}-DTA young (5 month) and aged (24 month) mice. Representative images of Pax7+ cells (white arrowheads) co-stained with DAPI. Scale bar = 100 μm. (**b**) Left panel: Quantification of satellite cell content in hind limb muscles in vehicle-treated mice. Right panel: Quantification of satellite cell content in hind limb muscles in tamoxifen-treated mice. Data are presented as mean satellite cells/fiber/cross-section (CS) ± SEM. (**c**) Mean fiber CSA of the hind limb muscles. Data are presented as mean fiber CSA ± SEM. N.S. – not significant ($P = 0.06$). n = 4–8 mice/group. * Significant effect of tamoxifen ($P < 0.05$), † Significant effect of age ($P < 0.05$) as measured by a two-way ANOVA (factors: young/aged and vehicle/tamoxifen).

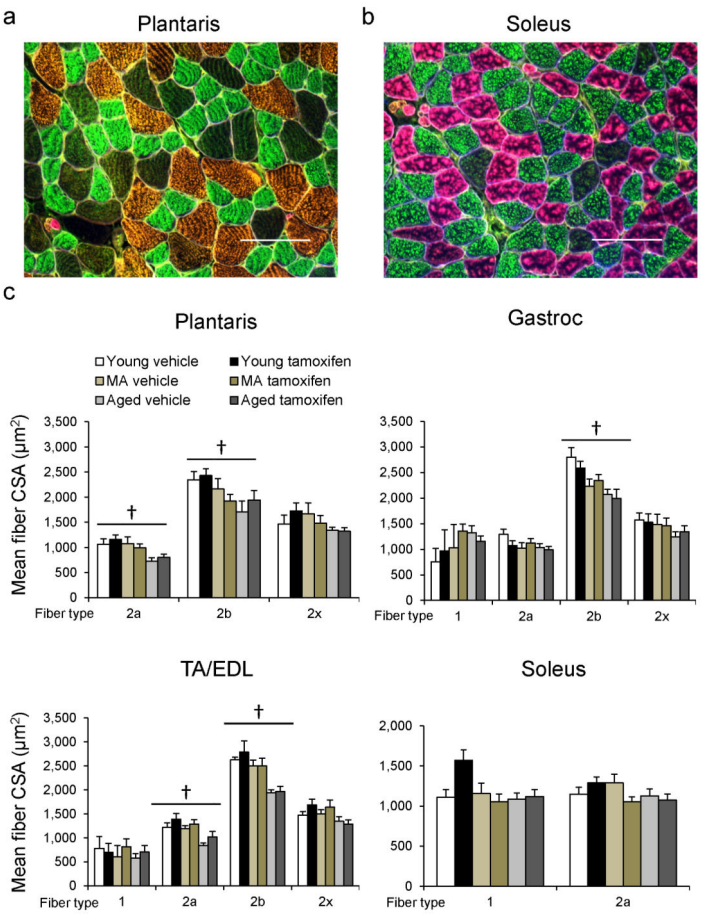

Figure 3. Age-associated fiber type-specific atrophy is unaffected by reduction in satellite cell content

Fiber-type specific cross-sectional area (CSA) of plantaris, gastrocnemius, TA/EDL and soleus muscles of vehicle- and tamoxifen-treated Pax7^{CreER}-DTA young (5 month), middle aged (MA, 16–18 month) and aged (24 month) mice. Representative images from plantaris (**a**) and soleus (**b**) showing myosin heavy chain type 1 (pink), 2a (green), 2b (orange) and 2x (unstained) fibers, in addition to dystrophin (white) ringing each fiber. Scale bar = 100 μm. (**c**) Quantification of mean CSA by fiber type in the hind limb muscles. Mean fiber CSA is provided for fiber types which comprise ≥ 2% of total fibers in a given muscle (see Supplemental Figure 1b for fiber type frequencies). Data are presented as mean fiber CSA ± SEM. n = 3–8 mice/group, † Significant effect of age ($P < 0.05$) as measured by a two-way ANOVA (factors: young/aged and vehicle/tamoxifen).

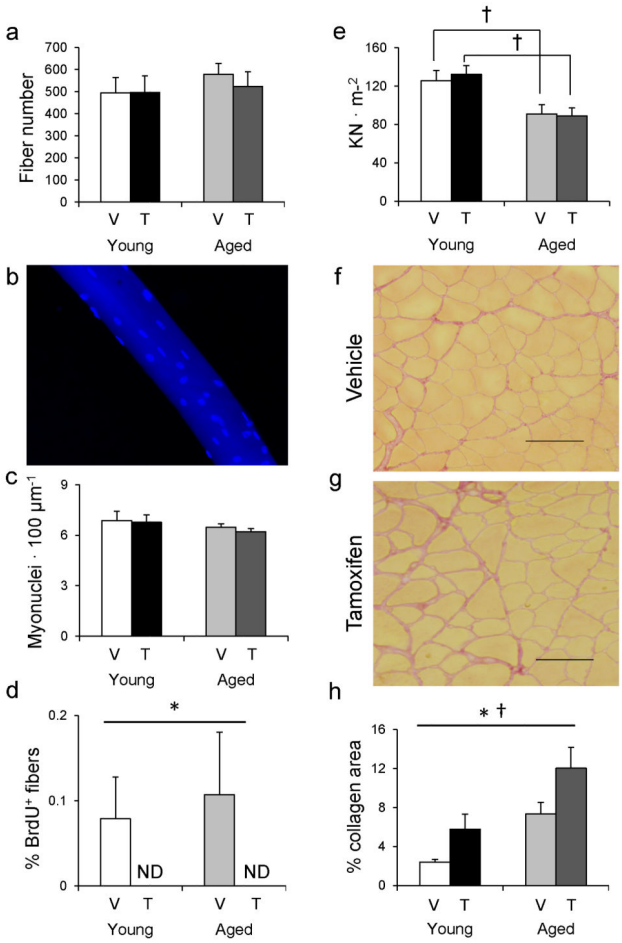

Figure 4. Reduced satellite cell content does not affect plantaris myofiber number, myonuclear number or single fiber force production during aging, but contributes to extracellular matrix (ECM) accumulation

Plantaris muscles isolated from young (5 month) and aged (24 month) $Pax7^{CReER}$-DTA vehicle- and tamoxifen-treated mice. (**a**) Number of myofibers in whole muscle cross-sections taken at mid-belly of the muscle. Data are presented as mean fiber number ± SEM. n = 5–7 mice/group. (**b**) Representative image of a single plantaris fiber with nuclei visualized with DAPI. (**c**) Myonuclear number normalized to myofiber length. Data are presented as mean number of myonuclei per 100 μm ± SEM. n = 40– 60 fibers/group. (**d**) Quantification of BrdU+/DAPI+ nuclei residing within the dystrophin antibody-labeled sarcolemma of myofibers. All fibers were counted in a cross section taken at mid-belly of the plantaris. Data are presented as % fibers BrdU+ ± SEM. n = 5–8 mice/group. (**e**) Maximum isometric force normalized to fiber cross-sectional area (specific force, KN/m^2) of permeabilized single fibers. Data are presented as mean specific force ± SEM. n = 5 Young vehicle, n = 7 Young tamoxifen, n = 6 Aged vehicle and n = 8 Aged tamoxifen; eight fibers/mouse. Representative images of vehicle- (**f**) and tamoxifen-treated (**g**) muscle stained with Sirius Red which binds collagens in the ECM. Scale bar = 100 μm. (**h**) Quantification of collagen content. Data are presented as mean % of total area ± SEM. n = 3–4 mice/group.

* Significant effect of tamoxifen ($P < 0.05$), † Significant effect of age ($P < 0.05$) as measured by a two-way ANOVA (factors: young/aged and vehicle/tamoxifen).